Vol. 38 (2007) ACTA PHYSICA POLONICA B No 2

SEARCH FOR TECHNIPARTICLES AT DØ*

Lorenzo Feligioni

Centre de Physique des Particules de Marseille
163, Av. de Luminy, 13288 Marseille, France

(Received November 15, 2006)

We search for the Technicolor process $\rho_\mathrm{T}/\omega \to \pi_\mathrm{T} W$ using events with one electron and two jets in 388 pb^{-1} of integrated luminosity recorded by the DØ experiment at Fermilab. As predicted by the Technicolor Straw Man Model (TCSM2) [K. Lane, S. Mrenna, *Phys. Rev.* **D67**, 115011 (2003)], π_T's decay dominantly into $b\bar{b}$, $b\bar{c}$, or $\bar{b}c$, depending on their charge. We select events containing b and c-quarks by identifying their secondary decay vertices within jets. We present two analysis methods based on topological variables, one is cut-based and the other using neural networks for separation of signal and backgrounds. In the absence of an observed excess above the standard model prediction for expected backgrounds we define an excluded region, as a function of ρ_T and π_T masses and a given set of model parameters.

PACS numbers: 12.60.Nz, 13.85.Rm

1. Introduction

Technicolor (TC), first formulated by Weinberg and Susskind [2, 3], is a non-Abelian gauge theory modeled after quantum chromo dynamics (QCD). TC provides a dynamical explanation of electroweak symmetry breaking by predicting a new strong SU(N_TC) gauge theory and new fermions, "techniquarks". Just as in QCD, in the low-energy limit of TC a spontaneous breaking of the chiral symmetry leads to breaking the electroweak interactions down to electromagnetism. The Nambu–Goldstone bosons produced in this process are called technipions π_T, in analogy with the pions of QCD. Three of these technipions become the longitudinal components of the W and Z bosons which acquire mass in the process.

An additional gauge field, Extended Technicolor [4, 5], couples standard model (SM) fermions and technifermions, producing a mechanism for generating quark and lepton masses. By imposing a particular dependence of TC

* Presented at the "Physics at LHC" Conference, Kraków, Poland, July 3–8, 2006.

coupling constants, Walking Technicolor [6] makes it possible to avoid the dangerous increase of the ordinary fermion coupling responsible for flavor-changing neutral currents. Still, to arrive at masses as high as the top quark mass, another interaction, Topcolor, is necessary, giving rise to Topcolor-assisted Technicolor models [7].

All the extensions of the basic Technicolor model require a large number $N_{\rm D}$ of technifermion doublets. In general, the Technicolor scale $\Lambda_{\rm TC}$ depends on the number of technifermion doublets $\Lambda_{\rm TC} \approx F_{\rm TC}/\sqrt{N_{\rm D}}$, where $F_{\rm TC}$ is the technipion decay constant. For large $N_{\rm D}$ the lowest lying technihadrons have masses on the order of few hundred GeV. This scenario is usually referred to as Low-Scale Technicolor.

In TCSM2, the parameter M_V controls the rate for $\omega_T \to \gamma + \pi^0_{\rm T}$ and is unknown *a priori*. Scaling from the QCD decay $\omega \to \gamma + \pi^0$ the authors of Ref. [1] suggest a value of several hundreds GeV. We set $M_A = M_V = 500\,\mathrm{GeV}$. The strength of technipions coupling to the SM particles depends on the mass of SM particle; $\pi_{\rm T}$'s in the mass range considered will decay most of the time into $b\bar{b}$, $b\bar{c}$, or $\bar{b}c$, depending on their charge.

2. Data event selection and modeling of signal and background events

In the DØ detector, described in [8], $W\pi_{\rm T}$ production can be identified by the presence of one isolated electron and missing transverse momentum ($\not{p}_{\rm T}$) from the undetected neutrino from the decay of the W boson, and two jets of hadrons coming from the fragmentation of the quarks from the decay of the technipion. We search for events with this signature in the data collected by DØ from April 2002 until July 2004. After requiring that at least one single electron trigger fired and good quality data, we are left with an integrated luminosity of $388\,\mathrm{pb}^{-1}$.

We select events in which there is exactly one well-identified electron based on tracking and calorimeter data with transverse momentum $p_{\rm T} >$ 20 GeV and pseudorapidity $|\eta| < 1.1$. To reject events with $Z \to ee$ decays, we require that there must not be any other electron candidates, with neither tracking nor pseudorapidity requirements, in the detector. We further require the presence of two jets with $p_{\rm T} > 20$ GeV and $|\eta| < 2.5$. We veto on the presence of any other jets in order to reduce the contamination from standard model processes with high jet multiplicity, such as $t\bar{t}$ or W+jets production. We accept all events with $\not{p}_{\rm T} > 20$ GeV and transverse mass $m_T > 30$ GeV calculated from electron $p_{\rm T}$ and $\not{p}_{\rm T}$. To further reduce backgrounds, we exploit the long lifetime of b-flavored hadrons. Tracks from decay products of b-hadrons may not project back to the proton–antiproton collision, but have a significant impact parameter. They can, therefore, be identified and used to reconstruct the decay vertex of the b-hadron. A jet is tagged as a b-jet if there is a secondary decay vertex within $\Delta R = \sqrt{(\Delta\eta)^2 + (\Delta\phi)^2} < 0.5$ from the jet axis. Our final Wjb data set of 117 events is defined by all selected events with at least one b-tagged jet.

We simulate the following standard model processes that contribute to the Wjb data set using different Monte Carlo generators and GEANT [9].

- Top-quark production: $t\bar{t}$ events have higher jet multiplicity than $W\pi_{\mathrm{T}}$ decays. They only produce the same signature, if one top quark decays to $e\nu b$ and some of the decay products of the other top quark are undetected. Single top-quark production is more likely to give rise to events that pass our final selection but it has a smaller cross section. Events with top quarks are generated using PYTHIA [10].

- $W(\to e\nu)$ + heavy flavor production: Events in which a W boson is produced together with two or more jets, at least one from the fragmentation of a heavy quark, are an irreducible source of background to this analysis. Among these processes are: W boson produced together with two b-jets ($Wb\bar{b}$), W plus one b-jet, and W plus at least one c-jet. $W + b\bar{b}$ production is generated and analyzed separately, all the others are referred to as W+heavy flavors. These processes are generated using ALPGEN [11].

- $Z(\to ee)$ + heavy flavor production.

- $W(\to e\nu) + Z(\to b\bar{b}$ or $c\bar{c})$ production.

Instrumental backgrounds arise from events in which objects are misreconstructed or misidentified. The QCD-multijet background is due to events with jets in which one or more jets are poorly measured, resulting in a substantial amount of missing momentum, and another jet fakes the electron signature. The W+jets background originates from events in which a light-quark or gluon jet is falsely identified as a b-jet. This contribution is estimated from the untagged W+jets data sample. The expected background event yields are listed in Table I.

We generate events with ρ_{T} masses between 155 GeV up to a maximum of 220 GeV. The π_{T} mass values start from the kinematic threshold for $W\pi_{\mathrm{T}}$ production at $M(\pi_{\mathrm{T}}) = M(\rho_{\mathrm{T}}) - M(W)$ up to $M(\pi_{\mathrm{T}}) = M(\rho_{\mathrm{T}})/2$ where the decay channel $\rho_{\mathrm{T}}^{\pm(0)} \to \pi_{\mathrm{T}}^{\pm,(0,\pm)}\pi_{\mathrm{T}}^{0,(0,\mp)}$ becomes accessible with the consequence of reducing the branching ratio of $\rho_{\mathrm{T}}^{\pm(0)} \to W\pi_{\mathrm{T}}$. We set $M(\omega_{\mathrm{T}}) = M(\rho_{\mathrm{T}})$ as suggested by the TCSM2 authors.

TABLE I

Estimated event yields in our final data set.

Process	Number of events
DATA:	117
Physics backgrounds:	
$t\bar{t} \to \ell\nu\ b\bar{b}\ q\bar{q}$	7.9
$t\bar{t} \to \ell^{+}\nu\ell^{-}\nu\ b\bar{b}$	14.1
$W^{*} \to tb \to (e\nu + \tau\nu)bb$	3.5
$qtb \to q\ (e\nu + \tau\nu)bb$	4.3
$W(\to e\nu) + b\bar{b}$	23.6
$W+$ heavy flavor	32.8
WZ	1.1
$Z(\to e^{+}e^{-})$	0.5
$Z(\to e^{+}e^{-}) + b\bar{b}$	0.6
Total physics backgrounds	88.5
Instrumental backgrounds:	
QCD-multijet	16.3
W + jets mistag	10.3
Total background:	115.1

3. Topological variables used for signal separation

The technicolor particles are expected to have narrow widths ($\approx 1\,\mathrm{GeV}$). We should, therefore, see enhancement in the distributions of dijet invariant mass $M(jj)$ and the invariant mass of the W boson-dijet system $M(Wjj)$.

We use the following kinematic variables to discriminate between signal and background.

- $\Delta\phi(j,j)$ is the difference in ϕ between the two jets in the event;
- $\Delta\phi(e,\not{p}_{\mathrm{T}})$ is difference in ϕ between the electron and the missing transverse momentum;
- $p_{\mathrm{T}}(jj)$ is the transverse momentum of the dijet system;
- H_{T}^{e} is the scalar sum of p_{T} of the electron and the two jets in the event;
- $M(j,j)$ is the invariant mass of the dijet system. This corresponds to the reconstructed π_{T} mass;
- $M(Wjj)$ is the invariant mass of the W boson-dijet system. This corresponds to the reconstructed ρ_{T} mass. We reconstruct the W boson from the electron and the missing transverse momentum using the W mass constraint to solve for p_z of the neutrino. If there are two real solutions, we take the smaller value of neutrino p_z. If there is only a complex solution, we take the real part.

Distributions for these variables are shown in Fig. 1. We use two approaches to separate signal and background, a cut based analysis and a neural network (NN) analysis.

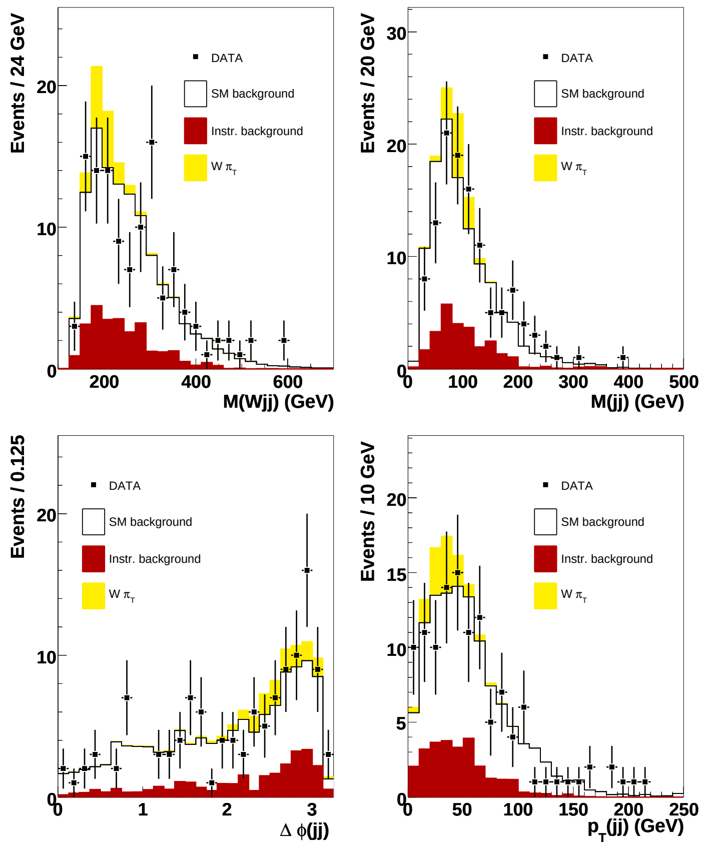

Fig. 1. Distribution for topological variables used for cut-based and NN analysis after Wjb selection. The white histogram represents the Standard Model prediction, dark (red) solid histogram represents the instrumental background, the light gray (yellow) histogram is the predicted $W\pi_{\mathrm{T}}$ signal for $M(\rho_{\mathrm{T}}) = 210\,\mathrm{GeV}$ and $M(\pi_{\mathrm{T}}) = 110\,\mathrm{GeV}$. Black dots are data.

4. Cut-based and neural network analyses

The cut-based analysis uses Monte Carlo simulations to maximize the $S/\sqrt{B}$ ratio, where S is the expected number of $W\pi_{\mathrm{T}}$ events and B is the expected number of background events, for every set of techni-particle masses after cutting on topological variables. The $S/\sqrt{B}$ ratio maxima determine a set of lower, upper or window cuts for each variable.

A two-stage neural network based on the Multi Layer Perceptron algorithm is also used. The layout of the first stage of this network consists of 8 input nodes and one hidden layer with 24 nodes, while the second stage has 3 input nodes and one hidden layer with 6 nodes. The inputs to the first stage of the network are the topological variables described above. This first stage consists of three independent networks which represent the different types of backgrounds: the Wjj network (includes both light quark and heavy flavor events), the $Wb\bar{b}$ network, and the top network (includes the $t\bar{t}$ and single top events). To train the network for the second stage, the three individual networks of the first stage are applied to each of the nine different physics backgrounds. For a given network from the first stage, these nine backgrounds are combined by weighting their respective contributions by the expected number of events as listed in Table I. We apply the neural network to the collider data, technicolor signals, physics and instrumental backgrounds to obtain the discriminator output spectrum shown in Fig. 2. We optimize the discriminator cut for every set of techniparticle masses to maximize $S/\sqrt{B}$.

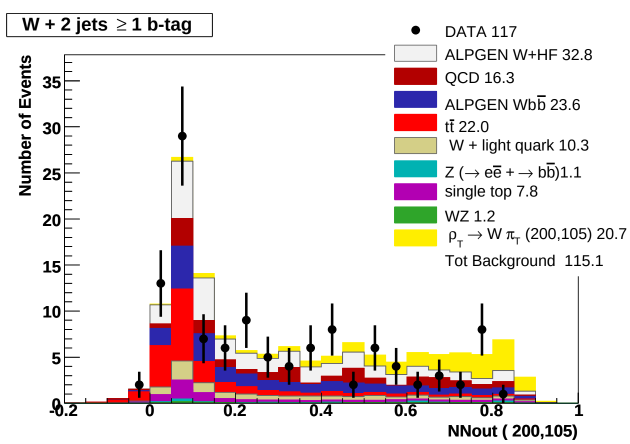

Fig. 2. Distributions of neural network output for signal and backgrounds. The top (yellow) histogram represents $W\pi_{\rm T}$ for $M(\rho_{\rm T}) = 200\,{\rm GeV}$, $M(\pi_{\rm T}) = 105\,{\rm GeV}$ and $M_V = 500\,{\rm GeV}$.

5. 95% C.L. upper limit on the cross section

In the absence of an excess over the expected background, we compute a 95% confidence level upper limit on the $\rho_{\rm T} \to W\pi_{\rm T} \to e\nu\; b\bar{b}(\bar{c})$ production cross section times branching ratio. In the cut-based analysis, which is a simple counting experiment, the limits are computed using Bayesian statistics [12]. The neural network analysis uses a 2-dimensional binned maximum likelihood technique to estimate the number of technicolor signal events by constraining the physics backgrounds and instrumental background contributions to the respective expectations within the statistical and systematic uncertainties. The regions excluded at 95% C.L. by both the cut-based and the neural network analyses in the $M(\rho_{\rm T}), M(\pi_{\rm T})$ plane, for $M_V = 500\,{\rm GeV}$ are illustrated in Fig. 3.

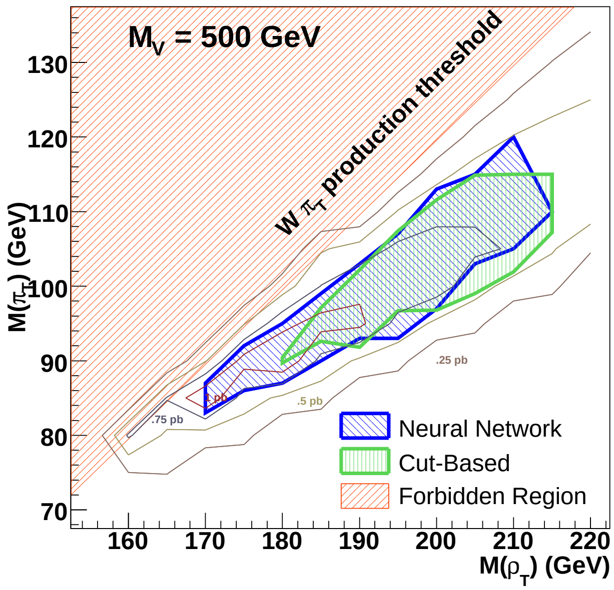

Fig. 3. Excluded region at 95% C.L. in the $(M(\rho_{\rm T}), M(\pi_{\rm T}))$ plane for $\rho_{\rm T} \to W\pi_{\rm T} \to e\nu\ b\bar{b}(\bar{c})$ production with $M_V = 500\,{\rm GeV}$ calculated using $388\,{\rm pb}^{-1}$ of DØ data with the cut-based analysis and with the neural network analysis. The diagonal line defines the kinematic threshold for $W\pi_{\rm T}$ production. The four iso-cross section curves indicate areas in the $M_{\rho_{\rm T}}, M_{\pi_{\rm T}}$ plane where the expected cross section times branching ratio is $\geq 1\,{\rm pb}$, $\geq 0.75\,{\rm pb}$, $\geq 0.5\,{\rm pb}$ and $\geq 0.25\,{\rm pb}$.

REFERENCES

[1] K. Lane, S. Mrenna, *Phys. Rev.* **D67**, 115011 (2003).
[2] S. Weinberg, *Phys. Rev.* **D13**, 974 (1976).
[3] L. Susskind, *Phys. Rev.* **D20**, 2619 (1979).
[4] S. Dimopoulos, L. Susskind, *Nucl. Phys.* **B155**, 237 (1979).
[5] E. Eichten, K. Lane, *Phys. Lett.* **B90**, 125 (1980).
[6] B. Holdom, *Phys. Rev.* **D24**, 1441 (1981).
[7] C.T. Hill, *Phys. Lett.* **345B**, 483 (1995).

[8] V.M. Abazov *et al.*, accepted by *Nucl. Instrum. Methods*, Fermilab-Pub-05/341-E, `physics/0507191`.

[9] R. Brun, F. Carminati, CERN Program Library Long Writeup W5013, 1993 (unpublished).

[10] T. Sjöstrand *et al.*, *Comput. Phys. Commun.* **135**, 238 (2001).

[11] F. Caravaglios, M.L. Mangano, M. Moretti, R. Pittau, *Nucl. Phys.* **B539**, 215 (1999).

[12] I. Bertram *et al.*, FERMILAB-TM-2104 (2000).